Electronic Supplementary Information

Synthesis of Flower-like Manganese Oxide for Accelerated Surface Redox Reactions on Nitrogen-Rich Graphene for Sustainable Aqueous Energy Storage

Jong Hyeong Lim[a,d,1], Jong Ho Won[b,1], Mun Kyoung Kim[c], Dae Soo Jung[d], Minkyung Kim[a], Chulhwan Park[e], Sang-Mo Koo[a], Jong-Min Oh[a], Hyung Mo Jeong[c], Hiesang Sohn[e,*] and Weon Ho Shin[a,*]

[a.] *Department of Electronic Materials Engineering, Kwangwoon University, Seoul 01897, Korea.*

[b.] *Department of Chemistry, Kookmin University, Seoul 02707, Korea.*

[c.] *School of Mechanical Engineering, Sungkyunkwan University, Suwon 16419, Korea.*

[d.] *Energy and Environment Division, Korea Institute of Ceramic Engineering and Technology (KICET), Jinju 52851, Korea.*

[e.] *Department of Chemical Engineering, Kwangwoon University, Seoul 01897, Korea*

[1.] *equal contribution*

* Corresponding Authors

E-mail: hsohn@kw.ac.kr, weonho@kw.ac.kr

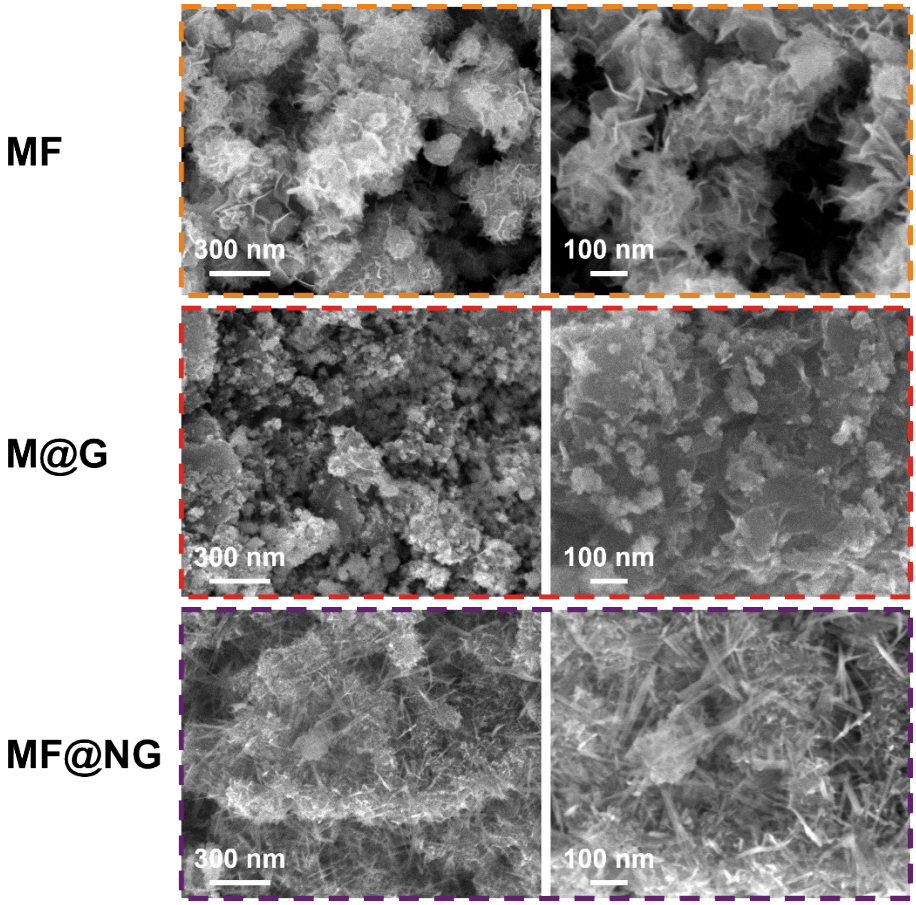

Figure S1. SEM images of MF, M@G, and MF@NG

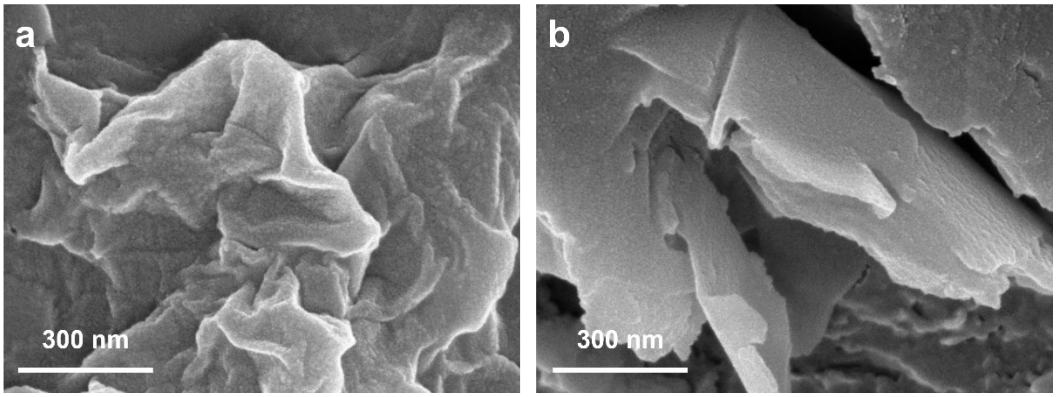

Figure S2. SEM images of a) GO and b) NGO

Table S1. Elements Analysis of GO and NGO.

	C (%)	H (%)	N (%)	S (%)	O (%)
GO	36.12	2.61	0.00	4.85	56.42
NG	66.14	1.66	10.36	0.04	21.80

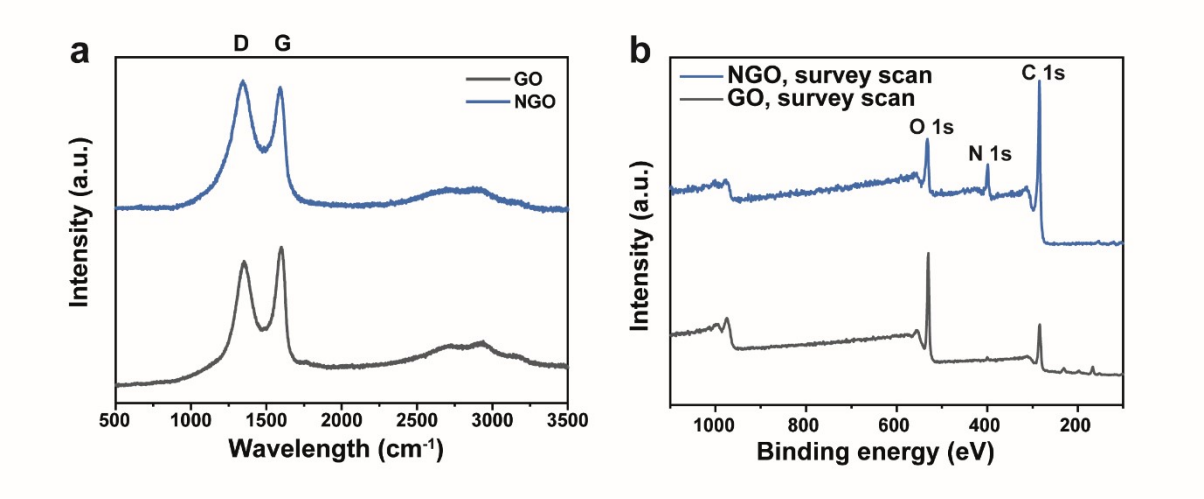

Figure S3. a) Raman spectroscopy of GO and NGO. b) XPS survey scan of GO and NGO.

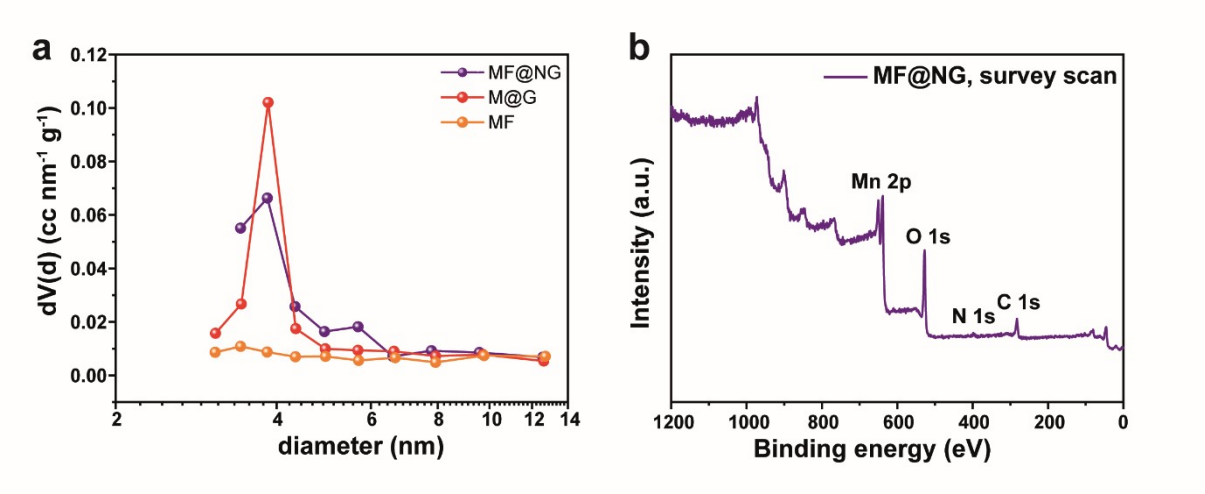

Figure S4. a) Pore distribution of MF, M@G, and MF@NG. b) XPS survey scan of MF@NG.

Table S2. Specific surface area, pore volume, and average pore diameter of MF, M@G, and MF@NG.

	MF	**M@G**	**MF@NG**
Specific surface area (m^2 g^{-1})	75.37	153.18	190.95
Pore volume (cm^3 g^{-1})	0.32	0.32	0.40
Average pore diameter (nm)	3.42	3.85	3.84

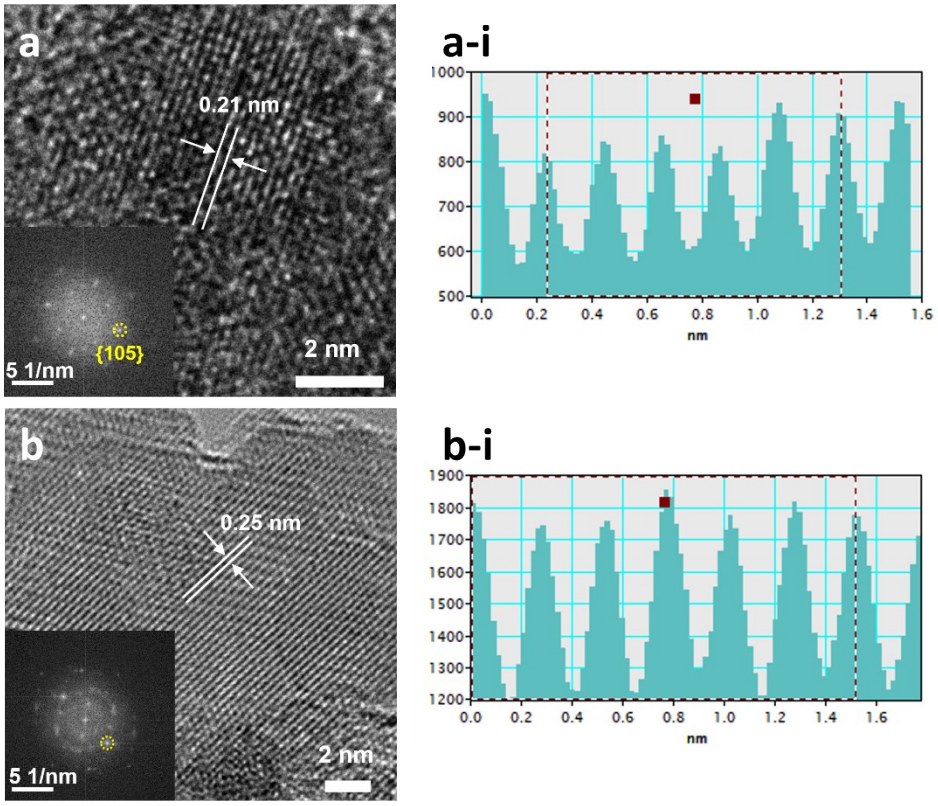

Figure S5. TEM image of MF@NG. a) High magnification TEM image of MF@NG sample with Mn_3O_4 part, and a-inset) FFT pattern of corresponding planes. a-i) Measuring d-spacing and corresponding profile plot of the calibration. b) High magnification TEM image of MF@NG sample with GO part, and b-inset) FFT pattern of corresponding plane. b-i) Measuring d-spacing and corresponding profile plot of the calibration.

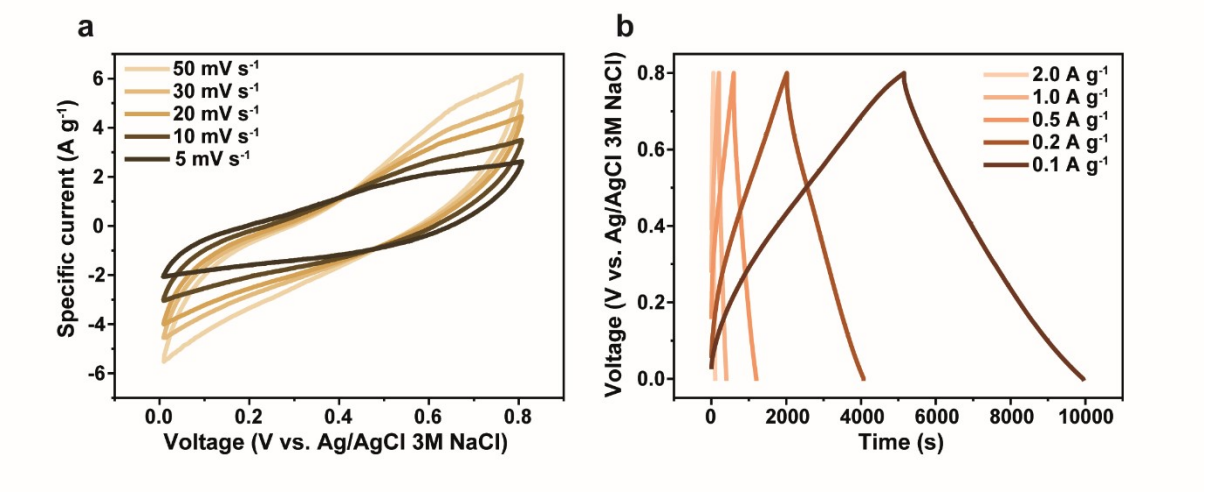

Figure S6. Electrochemical performance of MF electrode. a) CV curves with various scan rates of 5~50 mV s^{-1}. b) GCD curves at various specific current of 0.1–2 A g^{-1}.

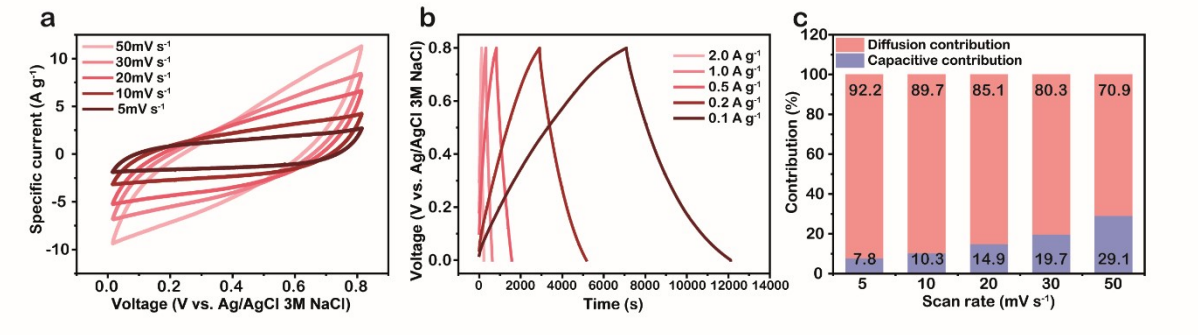

Figure S7. Electrochemical performance of M@G electrode. a) CV curves with various scan rates of 5~50 mV s^{-1}. b) GCD curves at various specific current of 0.1–2 A g^{-1}. c) Diffusion-, and capacitive-contribution reinterpreted from CV curves.

Table S3. Comparison of the electrochemical performance of the various Mn-oxide based materials

Materials	Voltage range (V)	Electrolyte	Specific capacitance (F g^{-1})	References
Bowl-like MnO_2 nanosheets	0–0.8	1M Na_2SO_4	379	[23]
MnO_2 nanorods electrode	0–0.8	0.5M Na_2SO_4	485	[24]
MnO_2 nanosheets	0–1.0	SiO_2-LiTFSI gel	243	[25]
Nitrogen doped graphene foam/carbon nanotube/manganese oxide	-0.2–0.8	1M Na_2SO_4	284	[26]
MnO_2/carbon nanotube/polyimide	0–1.1	CMC/Na_2SO_4 gel	543	[27]
Manganese oxide/carbon aerogel	0.1–0.9	0.5M Na_2SO_4	503	[28]
Reduced graphene oxide/MnO_2	0–1.0	1M Na_2SO_4	188	[29]
Mn_2O_3-carbon	-0.3–0.3	6M KOH	600	[30]
Porous MnO_2 nanosheets	0–0.9	0.5M $MgSO_4$	329	[31]
Potassium-containing manganese oxide	0–1.0	0.1M Na_2SO_4	234	[32]
Nitrogen doped graphene/Mn_3O_4	0–0.8	1M Na_2SO_4	654	[This work]

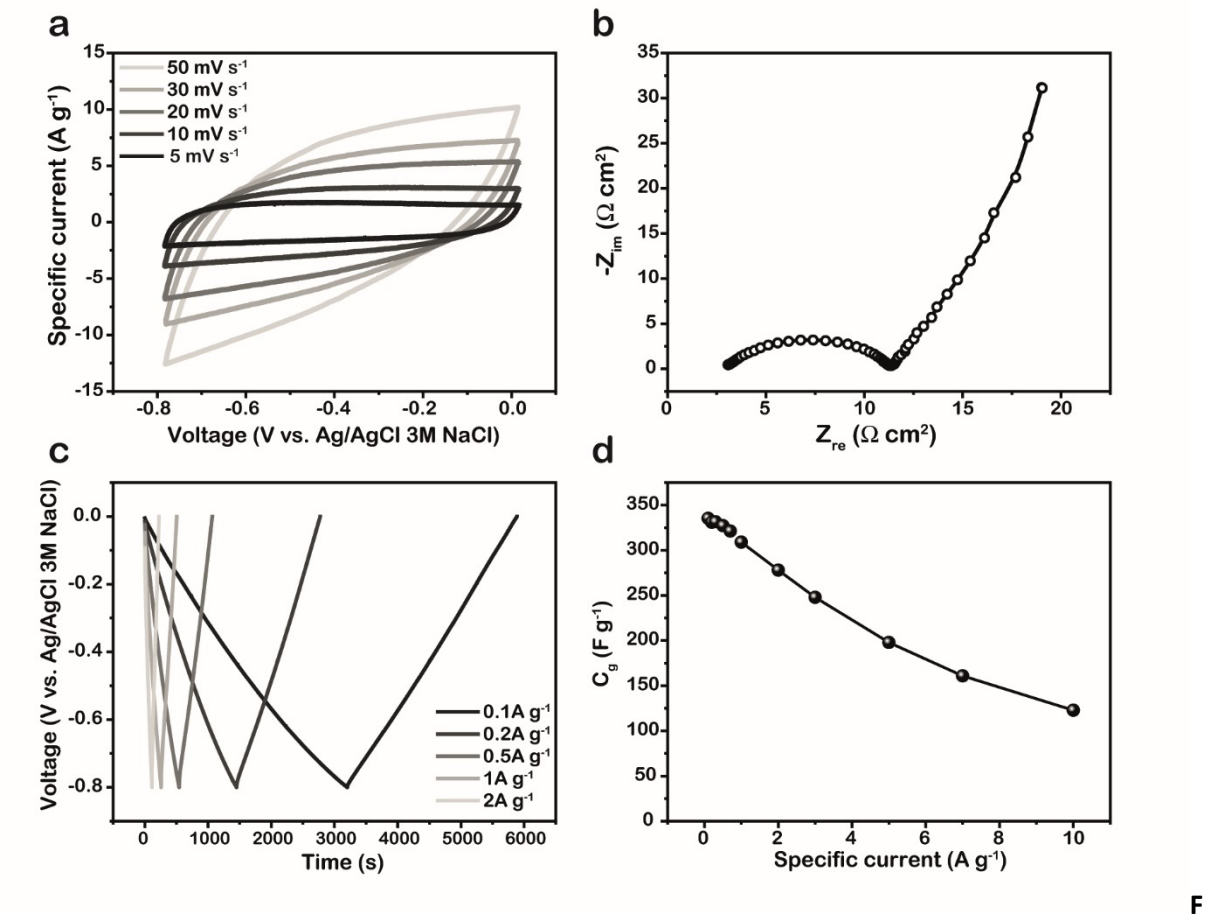

F

igure S8. Electrochemical performance of AC electrode. a) CV curves with various scan rates of 5-50 mV s^{-1}. b) EIS profile at frequency of 1 M-0.01 Hz with 5mV amplitude. c) GCD curves at various specific current of 0.1-2 A g^{-1}. d) Gravimetric capacitance reinterpreted from GCD curves.